Formation of Au fractal nanoclusters during pulsed laser deposition on highly oriented pyrolitic graphite

A. V. Zenkevich,* M. A. Pushkin, V. N. Tronin, V. I. Troyan, and V. N. Nevolin
Moscow Engineering Physics Institute, 31, Kashirskoe chausse 115409 Moscow, Russia

G. A. Maximov and D. O. Filatov
University of Nizhny Novgorod, 23, Gagarin Avenue 603950 Nizhny Novgorod, Russia

E. Lægsgaard
Institute of Physics and Astronomy, Århus University, DK-8000, Denmark
(Received 24 October 2001; published 1 February 2002)

The topography of the Au submonolayer condensate formed by pulsed laser deposition (PLD) on pyrolitic graphite surface has been studied by scanning-tunneling microscopy (STM). PLD technique is characterized by an extremely high instantaneous deposition rate (up to 10^{22} atoms $cm^{-2}s^{-1}$). The formation of Au fractal nanoclusters with $D=1.33\pm0.08$ was observed with STM. The mechanism driving the formation of fractal nanoclusters on the surface at high deposition rate is suggested to be the result of the interacting-adatom initial-states evolution in the system far from thermodynamic equilibrium. The geometrical structure of the forming nanoclusters depends critically on the rate at which atoms arrive at the surface as well as on its lattice symmetry.

DOI: 10.1103/PhysRevB.65.073406 PACS number(s): 81.15.Fg, 64.60.Ak, 68.37.−d

The concept of fractal geometry has got much attention in different fields of modern physics.[1,2] The nucleation of the new phase is one of the processes where fractal nature of the object often manifests itself. The formation of fractal clusters of (sub) micron size on the surface during submonolayer deposition utilizing the thermal-evaporation process (weakly nonequilibrium conditions) has been extensively studied (see Ref. 2 and references therein). This points at the specific mechanism of the solid-phase nucleation. The existing models describing the growth of fractal clusters at this scale such as diffusion-limited aggregation,[3] cluster-cluster aggregation,[4] Eden ballistic model[5] assume the presence of the spherical ''nucleus'' on which the dendritic structure, usually a microns in size, grows at the later stages.

The possibility of the formation of fractal metallic structures at the nanometer scale (the initial stage of nucleation) on the surface at the extremely high deposition rate was suggested in the work[6] while describing the peculiarities of Au nucleation on NaCl(100) during pulsed laser deposition (PLD). Until now, there is no full understanding of the role that highly nonequilibrium conditions play in the formation of fracatal clusters as well as of the link between the fractal dimension and the physics of the process. In this paper, we present the results of an experimental study on Au-nanocluster topography on a highly oriented pyrolitic graphite (HOPG) surface formed during the PLD process. We present experimental evidence that Au clusters of nanometer scale (~ 5 nm in size), nucleated on HOPG surface under highly nonequilibrium conditions, have fractal structure. We propose the mechanism driving the growth of fractal metallic nanoclusters under highly nonequilibrium thermodynamic conditions as a result of the formation of so-called connected Julia sets, which are known to have fractal boundaries.[7] The formation of fractal nanoclusters is believed to be the result of the evolution in the system of deposited atoms at the time scale when the information about the initial states of the system is not completely lost. At this time scale the discrete character of the atom's motion on the surface becomes important. Under these conditions the theory of discrete transformations of the complex plane in itself can be used, which gives rise to the emergence of fractal objects that are called Julia sets.[8] The proposed mechanism allows to describe qualitatively the observed pattern of the fractal clusters and to evaluate its dimension. The important feature of the proposed mechanism is that the fractal topography should vanish upon increasing the surface coverage. It appears that the shape and the dimension of clusters is determined by the rate at which atoms are arriving at the surface and by the symmetry of the substrate surface.

The clusters were formed by the PLD of Au on a freshly prepared HOPG surface at room temperature in ultrahigh vacuum (UHV) conditions at the base pressure $P\approx 5\times10^{-10}$ Torr. The surface quality prior to deposition was monitored *in situ* by Auger electron spectroscopy. The irradiation of YAG:Nd laser ($\lambda=1.06$ μm) with the energy $E=80$–200 mJ operating in the Q-switched regime ($t=15$ ns) with the repetition rate 25 Hz was focused on the Au target at the laser power density $P\approx10^{9}$ W cm^{-2}. The number of Au atoms deposited on the HOPG substrate in one pulse lasting $\tau_p\approx10^{-6}$ s was varied in the range 10^{13}–10^{15} atoms cm^{-2} (corresponding to the instantaneous deposition rate $j_{\mathrm{PLD}}=10^{19}$–10^{21} atoms $cm^{-2}s^{-1}$). The total amount of the deposited Au atoms for the fixed geometry and laser output energy was measured by Rutherford-backscattering spectroscopy (RBS) at $E_{\mathrm{He}}=2$ MeV. For comparison, thermally evaporated (TE) Au/HOPG samples at a similar Au coverage were also prepared. The deposition rate for TE was $j_{\mathrm{TE}}\approx10^{14}$ atoms $cm^{-2}s^{-1}$. The prepared Au/HOPG samples were investigated *ex situ* with scanning-

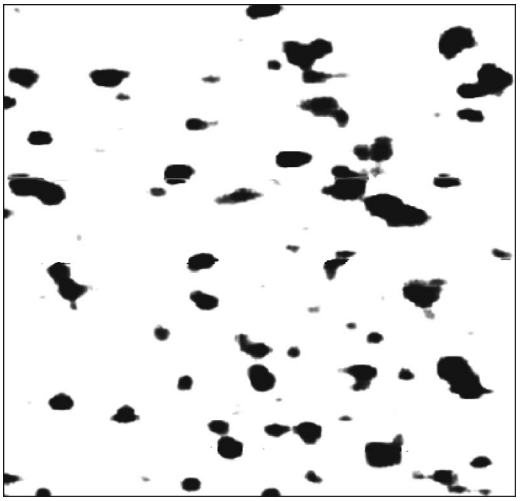

FIG. 1. STM image of Au nanoclusters formed on HOPG after one laser pulse ($n_{\mathrm{Au}} \simeq 1.3 \times 10^{14}$ atoms cm^{-2}). Scan area is 100 $\times 100$ nm.

tunneling microscopy (STM) using Omicron UHV AFM/STM LF1 micropscope. In principle, STM of Au/HOPG does not require an UHV environment and can be performed in ambient air. However, extreme stability of the employed instrument allows the recording of the topography in the constant-current mode at the slow scan rate (~ 0.5 line/s), which enables to analyze the shape of Au clusters down to atomic resolution. The $Pt_{0.8}Ir_{0.2}$ cut wire tips were employed. The tunneling current was ~ 0.8 nA, the gap voltage ~ 2–4 mV.

A STM image of Au clusters formed on HOPG after one laser pulse is shown in Fig. 1. According to RBS, this resulted in the deposition of $n_{\mathrm{Au}}^{\mathrm{PLD}} \approx 1.3 \times 10^{14}$ atoms cm^{-2}. The presented images were obtained by ''cutting'' the recorded scans at the level of 0.9 Å , relative to the graphite surface. On the HOPG surface, the adsorbed Au atoms occupy the sites in the center of carbon hexagons,[9] therefore, the number of adsorption sites n_0 on HOPG is $n_0 \simeq 5 \times 10^{14}$ cm^{-2}. Thus, the surface coverage θ was equal to $\theta = n_{\mathrm{Au}}^{\mathrm{PLD}}/n_0 \approx 0.25$. The topography of the deposit was analyzed using the well-known ''lake pattern'' algorithm,[10] where the relationship between two variables of the set of two-dimensional (2D) clusters—the area S vs perimeter p—is evaluated. If $S \sim p^{\nu}$ in double logarithmic scale is plotted, the straight line with the slope $\nu = 2$ ($S \sim p^2$) corresponds to the smooth nonfractal boundary, while $\nu < 2$ indicates the fractal structure of the boundary. The result of such analysis for PLD Au clusters is shown in Fig. 2. The values for individual clusters are fitted with the straight line with the slope $\nu = 1.5 \pm 0.1$ corresponding to the fractal dimension $D = 2/\nu = 1.33 \pm 0.08$.

For comparison, the similar scan for thermally evaporated Au/HOPG in the amount of $n_{\mathrm{Au}}^{\mathrm{TE}} \approx 5 \times 10^{14}$ atoms cm^{-2} is shown in Fig. 3. Although the atomic coverage is several times higher, the image exhibits smaller number of clusters, which are essentially 3D. The number of clusters on the scan is too few to make statistic analysis, therefore, the set of different scans was used and ''manual'' evaluation of S vs p

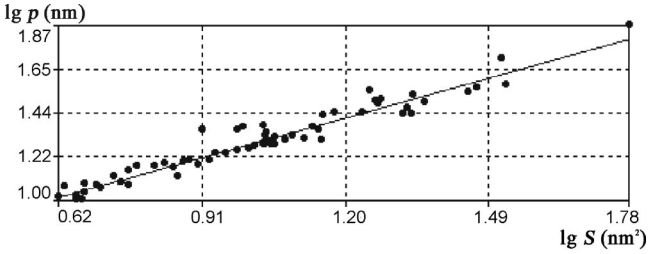

FIG. 2. The result of fractal analysis of pulsed-laser-deposited 2D Au clusters on HOPG (see Fig. 1). The slope of the straight line $\nu \approx 1.5 \pm 0.1$ corresponds to the fractal dimension $D = 2/\nu \approx 1.33 \pm 0.08$.

for sufficiently large number of clusters was performed. There is no surprise that for Au clusters formed on HOPG in the thermal-evaporation process, the linear fit points at the slope $\nu \approx 1.95 \pm 0.05$, which corresponds to the nonfractal shape of clusters.

The main difference between PLD and TE with respect to the nucleation process is believed to be the rate at which atoms are arriving at the surface during deposition and nucleation of the condensed phase. For TE at the typical deposition rate $j_{\mathrm{TE}} \approx 10^{14}$ atoms $\mathrm{cm}^{-2}\,\mathrm{s}^{-1}$ the adatom during its lifetime on the surface $\tau_{ad} \approx 10^{-4}$ s [$\tau_{ad} = \tau_0 \exp(\varepsilon/kT)$, $\tau_0 \approx 10^{-13}$ s, $\varepsilon \approx 0.6$ eV, $T = 300$ K] can make some $m = \tau_{ad}/\tau_1 \sim 10^5$ elementary jumps [$\tau_1 \approx a^2/\mathcal{D} \simeq 3 \times 10^{-10}$ s is the time of elementary jump, $a \simeq 5$ Å is the lattice parameter, $\mathcal{D} \approx 1 \times 10^{-5}$ $\mathrm{cm}^2\,\mathrm{s}^{-1}$ is the surface diffusion coefficient of metal adatom on HOPG at RT (Ref. 11)]. As the concentration of adatoms $n_{ad} = j\tau_{ad}$ reaches the value $n_{ad} \geqslant n_{\mathrm{sat}}$ (n_{sat} is the surface concentration of adatoms in the saturated two-dimensional gas), the condensate is forming. The described mechanism of the new phase nucleation represents the classical Volmer-Weber-Zel'dovich model.[12] As was mentioned above, PLD is characterized by a very high (instantaneous) deposition rate ($j_{\mathrm{PLD}}/j_{\mathrm{TE}} \simeq 10^7$). The relaxation of adatoms' system at such deposition rate is set by the initial conditions and occurs through the motion of each particle to the state defined by the minimum of energy (the motion towards the attractor). The formation of the attractor

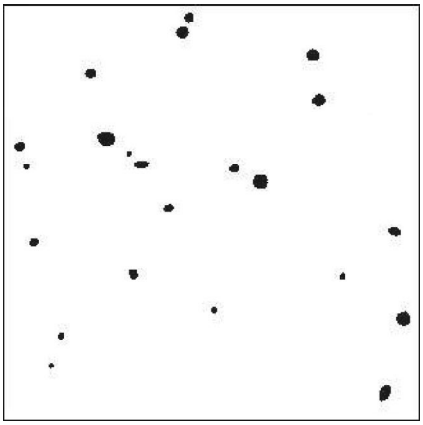

FIG. 3. STM image of Au clusters on HOPG formed by thermal evaporation ($n_{\mathrm{Au}} \simeq 5 \times 10^{14}$ atoms cm^{-2}). Scan area is 100 $\times 100$ nm.

occurs at the critical coverage $\theta_c \simeq n_c/n_0$, which is achieved at the time $\tau_c = n_c/j_{\mathrm{PLD}}$ and corresponds to the average distance between adatoms $r \simeq n_c^{-1/2}$. It results in the motion of adatoms towards the attractor from the area affected by the attractor. The size of this zone d depends on the interaction of adatoms and can be estimated in the mean-field approximation as the size of 1–2 coordination spheres, $d \simeq (2-4)r$. The motion of adatoms towards the attractor, meaning the formation of the cluster, takes the time $\tau_m \simeq d^2/4\mathcal{D}$. This process is maintained if during the time τ_c the arrival of the new portion of atoms at the same area is provided, i.e., if $\tau_m \geqslant \tau_c$. Otherwise, the concentration of adatoms in the zone of the attractor falls lower than θ_c and the process ceases. The critical coverage can be estimated from the equilibrium condition $\tau_m = \tau_c$: $\theta_c \simeq (j_{\mathrm{PLD}}/\mathcal{D})^{1/2}/n_0 \simeq 0.02$, which corresponds to the time of the cluster formation $\tau_m \simeq 10^{-8}$ s and the size of the attractor zone, $d \simeq 40$–120 Å. It means that atoms make some ten elementary jumps before reaching the attractor.

For quantitative description of the proposed mechanism of cluster formation let us consider an equation for the particle's motion in the mean-field approximation,

$$\dot{\vec{r}} = -\Gamma \frac{\partial U}{\partial \vec{r}}, \tag{1}$$

where $\vec{r}$ is the radius vector of the particle, $\Gamma \simeq \mathcal{D}/T$ is the mobility, U is the potential energy of the particle. $U = U_1 + U_2$, where $U_1(n, |\vec{r}|)$ is the energy of the self-consistent field of all particles, which is defined by the number of nearest neighbors (NN) and U_2 is the energy of crystalline field representing the symmetry of the crystalline lattice on the surface. At the time scale $\tau \geqslant \tau_1$ the atom motion on the surface is stepwise, therefore, in Eq. (1) one should go over into the discrete representation. Then, it takes the form

$$\vec{r}_{k+1} = \vec{r}_k - \tau_1 \Gamma \frac{\partial U(\vec{r}_k)}{\partial \vec{r}_k}. \tag{2}$$

The self-consistent field of deposited atoms U_1, which affects the given atom can be represented as $U_1 = Zf(\vec{r}_k - \overline{\vec{r}})$, where Z is the number of NN for this atom, f is the energy of atoms pair interaction, $\overline{\vec{r}}$ is the average distance between adatoms. Taking into account the surface symmetry about the rotation for the angle $2\pi/q$,[13] Eq. (2) in the complex representation can be reduced to the form

$$z_{k+1} = Az_k + B(z_k^*)^{q-1},$$

$$A = 1 - \tau_1 \Gamma (\theta n_0)^{-1/2} \frac{\partial U_1}{\partial |z|}\Big|_{(\theta n_0)^{-1/2}}, \tag{3}$$

where B is the constant expressing the binding energy of atom with the substrate. Expression (3) is the reflection of the complex plane in itself. It is known[7] that the images of this kind of reflections are fractal, the boundaries of such areas are the so-called Julia sets. At certain conditions on the surface (θ, T, q) atoms that find themselves in the area that is limited by the Julia set will move towards attractor, thus forming a cluster. Atoms that are out of this area will move away from the attractor. In other words, the energetic regions described by Julia sets emerge on the surface and the behavior of each adatom is described by its initial conditions. This corresponds to the initial stages of the evolution of the nonequilibrium system's strongly correlated states. It is important to note that such energetic areas are true (mathematical) fractals, which are self-similar at any scale. The model assumes that the structure of the real cluster should, to some extent, reproduce the fractal structure of Julia set. However, due to the finite size of the atom such an object cannot be a true mathematical fractal.

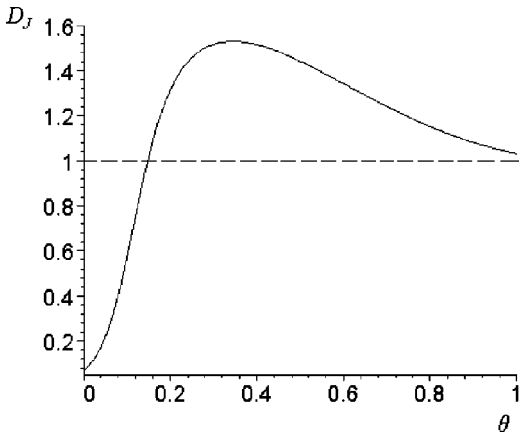

FIG. 4. The fractal dimension D_J of the calculated energetic areas on HOPG surface as a function of the surface coverage by Au atoms, θ (see the text).

Let us assume now that the dimension of the physical cluster is the same as that of the ''parent'' Julia set (D_J). The calculation of the fractal dimension of the Julia set for the reflection of the form (3) was performed numerically using the renormalization Schroeder equation.[7] The dimension D_J versus coverage θ plot shown in Fig. 4 is calculated with the following parameters: the energy of interaction of Au atoms with each other $\varepsilon_{\mathrm{Au\text{-}Au}} = 0.3$ eV and with the substrate $\varepsilon_{\mathrm{Au\text{-}C}} = 0.4$ eV, $T = 300$ K, and $q = 3$, which corresponds to the Au/HOPG system. At low coverage $D_J < 1$, i.e., the Julia set is not connected. It means that at such θ, under high deposition rate, the aggregation of adatoms on the surface does not occur. The dimension D_J increases with the coverage achieving $D = 1.54$ at $\theta \approx 0.35$ and the structure of the forming clusters is defined by the structure of the emerging energetic areas of the corresponding dimension. Further increase of the coverage θ results in the decrease of the fractal dimension D_J. The sequence of Julia sets for several values of parameter θ is shown in Fig. 5. One can see that as the coverage is increasing, the boundaries of the energetic zones (Julia sets) are becoming more smooth. STM images of experimentally observed Au clusters on HOPG are also shown in Fig. 5.

Unfortunately, the experimental verification of the predicted evolution of the clusters fractal structure as a function of the surface coverage is difficult to perform for the Au/HOPG system. Though 2D growth mode of Au clusters on

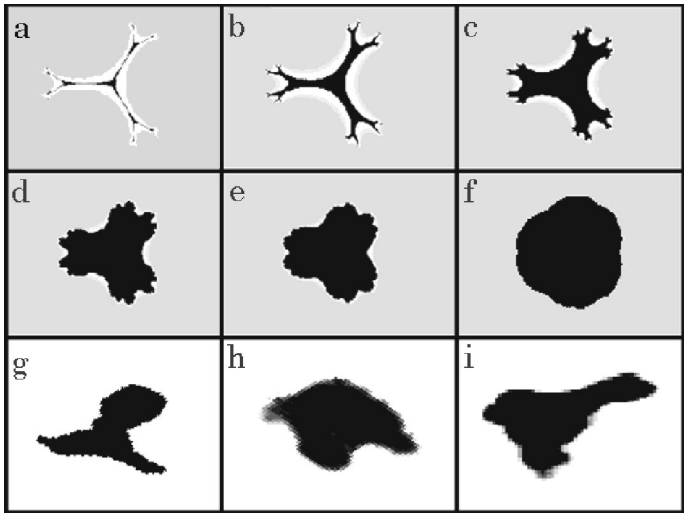

FIG. 5. The sequence of filled Julia sets for different coverage values: (a) $\theta=0.1$, $D_J=0.54$, (b) $\theta=0.15$, $D_J=1.06$, (c) $\theta=0.2$, $D_J=1.24$, (d) $\theta=0.3$, $D_J=1.43$, (e) $\theta=0.35$, $D_J=1.54$, and (f) $\theta=0.8$, $D_J=1.01$ compared to STM images of real Au clusters on HOPG [scan area is (g) 20×16 nm, (h) 10×8 nm, and (i) 9×7 nm].

HOPG during PLD is an advantage while investigating the geometric structure of clusters by STM, it turns to be a drawback as soon as individual clusters begin to coagulate on the surface and consequently the topological analysis of isolated clusters becomes impossible to perform. Nevertheless, the analysis of the experimental samples for four and ten laser pulses corresponding to the total amount of deposited metal, $n_4=4.7\times10^{14}$ atoms cm^{-2} and $n_{10}=1.75\times10^{14}$ atoms cm^{-2}, respectively, showed that clusters formed in these conditions also have a fractal structure with the dimension $D_4=1.35\pm0.05$ and $D_{10}=1.42\pm0.05$. Although the presented model does not predict the evolution of cluster structures upon further deposition ($N>1$), these results corroborate the general character of the observed phenomenon.

In conclusion, unlike the thermal-evaporation process, the nanoclusters with fractal structure are forming as a result of PLD of Au onto the HOPG surface as revealed with STM. The formation of fractal nanoclusters on the surface at high deposition rate is suggested to be the result of evolution of the interacting-adatom initial states in highly nonequilibrium system. The proposed model claims that the fractal structure of the forming nanoclusters depends critically on the rate at which atoms arrive at the surface as well as on its lattice symmetry and vanishes while the size of the clusters increases.

The work has been supported in part by the Joint Russian-American Program ''Higher Education and Basic Research'' sponsored jointly by the US Civilian Research and Development Foundation (CRDF) and the Russian Ministry of Education, Project No. REC-001.

*Electronic address: zenkevich@t103.mephi.ru

[1] O. Malcai, D. A. Lidar, O. Biham, and D. Avnir, Phys. Rev. E **56**, 2817 (1997).
[2] A.-L. Barabasi and H. E. Stanley, *Fractal Concepts in Surface Growth* (Cambridge University Press, Cambridge, 1995), Chap. 17.
[3] T. A. Witten and L. M. Sander, Phys. Rev. B **27**, 5686 (1983).
[4] *Aggregation and Gelation*, edited by F. Family and D. P. Landau (North-Holland, Amsterdam, 1984).
[5] D. N. Sutherland, J. Colloid Interface Sci. **22**, 300 (1985).
[6] V. D. Borman, A. V. Zenkevich, S. Ch. Lai, V. N. Nevolin, M. A. Pushkin, V. N. Tronin, V. I. Troyan, and J. Chevallier, JETP Lett. **72**, 148 (2000).
[7] J. Milnor, *Dynamics in One Complex Variable* (Friedr. Vieweg & Sohn Verlagsgesellschaft Mbh, Wiesbaden, 1999).
[8] H.-O. Peitgen and P. H. Richter, *The Beauty of Fractals: Images of Complex Dynamics Systems* (Springer-Verlag, Berlin, 1986).
[9] T. Endo, T. Sumomogi, H. Maeta, S. Ohara, and H. Fujita, Mater. Trans., JIM, **40**, 903 (1999).
[10] J. M. Gomez-Rodriguez, J. Vac. Sci. Technol. B **9**, 495 (1991).
[11] G. M. Francis, L. Kuipers, J. R. A. Cleaver, and R. E. Palmer, J. Appl. Phys. **79**, 2942 (1996).
[12] E. M. Lifshitz and L. P. Pitaevskii, *Physical Kinetics* (Pergamon, Oxford, 1981).
[13] V. I. Arnold, *Geometrical Methods in the Theory of Differential Equations* (Scientific Research Center R&C Dynamics, Izhevsk, Russia, 2000).